

Jian Zhang¹, Shunxin Wang¹, and Beth Clarke¹

¹Cooperative Institute for Mesoscale Meteorological Studies, University of Oklahoma, Norman, OK

1. INTRODUCTION

WSR-88Ds (Weather Surveillance Radar – 1988 Doppler) can detect both meteorological and non-meteorological scatters. The non-meteorological scatters include ground and sea clutter due to normal or anomalous radar beam propagation, biological targets such as birds and insects, electronic interferences, etc. Power returns from these scatters can contaminate radar observations and cause users to misinterpret the data. Moreover, contaminated radar data will have negative impacts on downstream applications and weather products such as precipitation estimations.

Some clutter suppression procedures have been implemented in radars' signal processing before base level data are disseminated to users. However significant non-meteorological echoes often remain after the clutter suppression. To remove the non-meteorological echoes, many different approaches have been suggested. A complete review of the approaches can be found in Steiner and Smith (2002). Generally, spatial (horizontal and vertical) variations of reflectivity, velocity and spectrum fields are analyzed and different types of echoes are identified based on various features in the variations. For instance, intensity and texture of reflectivity fields along with other features in velocity and spectrum width fields are used as inputs to fuzzy logic (Kessinger et al. 2003) and neural network (Lakshman 2003) procedures. Steiner and Smith (2002) found that most useful parameters are the vertical extent of radar echoes, the horizontal variability of reflectivity field, and the vertical gradient of reflectivity. However, since the parameters in Steiner and Smith (2002) were computed with respect to radar tilts, their technique could remove shallow precipitation at far ranges yet retain some clear air returns and clutter at close ranges.

In this paper we present a new technique that uses vertical parameters similar to those in Steiner and Smith (2002) but the parameters are computed with respect to height instead of to radar tilts. By using the physical height, the impact of beam spreading on the algorithm can be significantly reduced. The horizontal variability parameter used in the new technique is the texture of reflectivity (Kessinger et al. 2003).

In the next section, Sect. 2, the methodology of the reflectivity QC algorithm is presented. Example results of the QC algorithm for various cases are shown in section 3. A summary is given in section 4.

2. METHODOLOGY

2.1 Characteristics Of Different Echo Types

Radar reflectivity observations contain two important classes: precipitation and non-precipitation echoes. There are three major types of non-precipitation echoes in reflectivity fields. The first type of non-precipitation echoes is from insects, birds, dust, chaff and other particulates in the atmosphere that are large enough to return some power to the radar. The second type is ground clutter echoes caused by radar beams hitting buildings and mountains, or sea clutter echoes caused by radar beams hitting oceanic waves. The third type of non-precipitation echoes is ground or sea clutter under special atmospheric refractive index conditions where radar beams propagate in a path that bends downward toward the earth's surface. This is so called "abnormal propagation (AP)" situations in radar meteorology. The normal propagation path of radar beams is usually bending upward with respect to the earth's surface.

The non-precipitation echoes of first type (except for chaff) are usually below 3 km above ground level. Furthermore, these echoes associated with biological targets and dust are usually weak in intensity (less than 35dBZ) and contain small horizontal scale noises in reflectivity fields. Ground and sea clutter echoes, either from normal or anomalous propagations, are usually correlated with terrain/ocean and are usually in the lower tilts of radar observations.

Precipitation echoes can be classified into two groups: convective and stratiform. Convective precipitation systems are typically associated with high rain rates and strong horizontal reflectivity gradients, and they usually have smaller horizontal scales than do stratiform precipitation systems. Convective precipitation echoes have large vertical scales that usually extend above 5 km above ground level. The large vertical depth of convective precipitation echoes makes it relatively easy to distinguish them from the non-precipitation echoes.

*Corresponding Author address: Jian Zhang, 1313 Halley Circle, Norman, OK 73069; e-mail: jian.zhang@noaa.gov.

Stratiform precipitation echoes are characterized by light to moderate rain rates, weak horizontal reflectivity gradients, and large aerial coverage (usually greater than 500 km²). It is not uncommon that stratiform precipitation cloud tops are below 4.5 km or even 3 km above ground level (AGL). The shallowness of these stratiform precipitation echoes sometimes makes it difficult to distinguish them from the non-precipitation echoes. However, stratiform precipitation is relatively uniform in space and the associated reflectivity fields are usually very smooth horizontally. Since majority of the non-precipitation echoes contain small-scale noises in reflectivity fields, a criteria related to the horizontal smoothness of reflectivity field would help identify stratiform precipitation against non-precipitation echoes. It is noteworthy, though, that sometimes AP echoes, such as those in a flat terrain region under severe super refractive atmospheric conditions, can have very smooth horizontal reflectivity fields. In this situation, the AP echoes are not readily separated from stratiform precipitation echoes and additional criteria need to be used for accurate identification of the AP echoes. One such criterion is the aerial extent of the echoes. As mentioned before, the stratiform precipitation usually extends 100s to 1000s km². AP echoes, except for rare occasions, are usually localized and have little continuity in azimuth direction. Therefore a neighborhood continuity check can help identify and remove some of the AP echoes.

2.2 Procedures Of The Reflectivity QC Algorithm

Figure 1 shows an overview flowchart of the new reflectivity QC algorithm. Detailed descriptions of each step are given in the following.

2.2.1 Noise filter

The input data to the reflectivity QC algorithm is a volume of 3D reflectivity field on a spherical grid (range, azimuth and elevation). A simple filter is applied to the raw reflectivity field to remove isolated reflectivity points or lines. For any given reflectivity bin, X , the number (N) of non-missing reflectivity observations is counted in a box of 5×5 bins that is centered at the given bin. The percentage (P_x) of non-missing values in the box is then calculated by:

$$P_x = N/N_{total} \quad (1)$$

Here N_{total} (= 25) represents the total number of bins/pixels in the box. If P_x is less than a given threshold (default value = 75%), then the pixel X is considered an isolated point and is removed. The filter is shown to be very effective in removing speckle echoes (Fig.2).

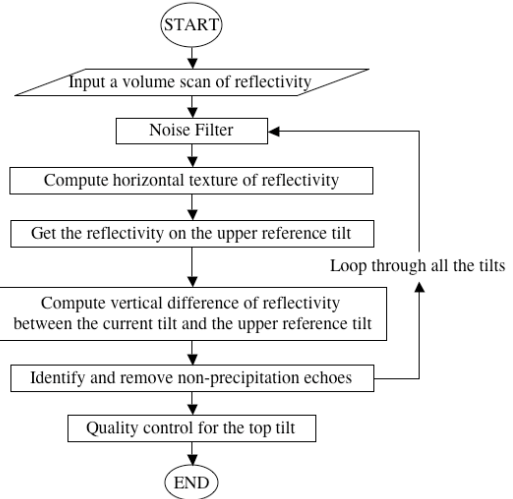


Fig. 1 Flowchart of the reflectivity QC algorithm

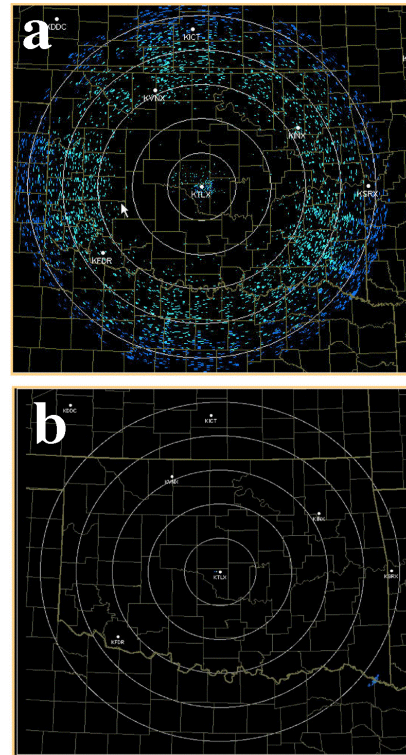


Fig. 2 An example 0.5° tilt reflectivity field before (a) and after (b) the noise filter.

2.2.2 Horizontal reflectivity texture

The horizontal smoothness of reflectivity fields is measured by a parameter called texture of reflectivity ($TDBZ$, Kessinger et. al., 2003). It is the mean square difference between adjacent reflectivity values along a radial. The formula for computing $TDBZ$ at a given bin is:

$$TDBZ = \frac{\sum_{j=1}^{ngates} \sum_{i=1}^{nrays} (Z_{i,j} - Z_{i,j-1})^2}{N} \quad (2)$$

Here i and j are indices of reflectivity bins in azimuth and range directions, respectively. Z represents reflectivity values in dBZ; $nrays$ and $ngates$ are number of bins in a box centered at the given bin; $N = nrays \times ngates$ represents total number of bins in the box. The default values for $nrays$ and $ngates$ are 7.

Figure 3 shows example reflectivity and the associated $TDBZ$ fields for a squall line case. The reflectivity field is from the 0.5° tilt. Large $TDBZ$ values are associated with the convective cells as well as with the AP clutter echoes behind the squall line. Therefore, by texture parameter itself one cannot distinguish between precipitation and non-precipitation echoes accurately.

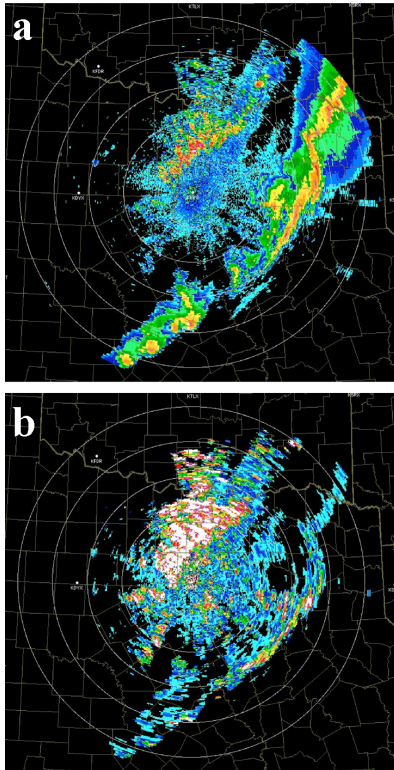


Fig. 3 An example $TDBZ$ field (b) and the associated base reflectivity field (a) on 0.5° tilt.

2.2.3 The upper reference tilt

As discussed in section 2.1, most of convective precipitation and many stratiform precipitations have cloud tops exceeding 3 km above the ground level. Non-precipitation echoes, except for chaff echoes, however, are usually contained in the lowest 3 km of the

atmosphere. Thus the vertical continuity of reflectivity at and above 3 km above ground level becomes a very useful criterion to distinguish precipitation from non-precipitation echoes. For some shallow stratiform precipitation echoes, additional criteria such as reflectivity texture field will be used to prevent false removal of precipitation echoes.

In the present QC algorithm, the vertical scale of echoes is represented by a parameter called vertical difference of reflectivities (VDZ). The VDZ is the difference between a reflectivity at a given gate on the tilt that is under QC and a reflectivity at the same gate on an upper tilt that intersects any height between 3 and 4.5 km above the radar level. Note that different tilts intersect a constant height level at different ranges. For instance, at the range of 30 km the 3 km above radar level (ARL) height intersects the 6th tilt (6° elevation angle) for VCP 21 (Fig. 4). At the ranges of 90 and 160 km, the 3 km ARL height intersects the 2nd (1.45° elevation angle) and 1st (0.5° elevation angle) tilts, respectively (Fig. 4). For certain gates, there are no corresponding upper tilts exactly intersects with 3 km ARL height. Under these circumstances, slightly higher height values (up to 4.5 km ARL) are used to find an upper reference tilt so that the VDZ parameter can be obtained. Since the operational WSR-88Ds scan in pre-specified elevation angles, the upper reference tilt indices associated with the 3 – 4.5 km ARL height level can be pre-determined for each gate. This set of gates on different tilts make up a hybrid tilt which will be referred as “upper reference tilt” (URT) hereafter. Note that different VCPs generally have different upper reference tilts.

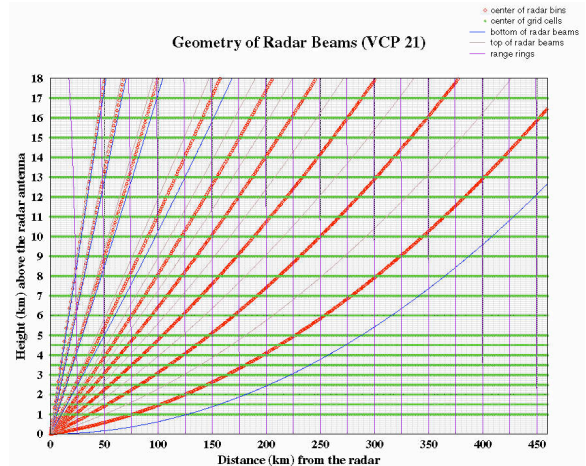


Fig. 4 Radar beam propagation paths (height versus range) under standard atmospheric refraction conditions.

In the current QC algorithm, the VDZ is calculated for each gate by subtracting the reflectivity value at a gate on the tilt under QC by the reflectivity value at the same gate on the upper reference tilt. Before VDZ is

computed, reflectivity values on the upper reference tilt are pre-processed. The purpose of the pre-process is to identify apparent non-precipitation echoes on the upper reference tilt using a tilt-to-tilt vertical check and horizontal reflectivity texture check.

2.2.4 Vertical difference of the reflectivity and non-precipitation echo removal

The vertical difference of the reflectivity (VDZ) field is calculated as the following:

$$VDZ = (Z - Z_{URT}^a) / (H_{URT} - H) \quad (3)$$

Here Z is the reflectivity value under examination; Z_{URT}^a is the pre-processed reflectivity value on the upper reference tilt. H and H_{URT} are the heights associated with the two reflectivities Z and Z_{URT}^a , respectively. The unit of VDZ is dBZ/km and it is set to missing when either Z or Z_{URT}^a are missing. If VDZ value at any given gate is larger than a threshold (default value = 20.0 dBZ/km), then the reflectivity observation at the gate is considered a non-precipitation echo and the reflectivity value will be replaced by a missing flag.

Figure 5 shows an example VDZ field and the associated base reflectivity field at the 0.5° elevation angle. The small VDZ values are associated with the precipitation areas in the squall line, while the large VDZ values are well correlated with the AP clutter behind the squall line. Therefore the VDZ parameter is a very good parameter for separating precipitation and non-precipitation echoes in this case.

The VDZ field can only be obtained for the gates within certain range from the radar. This is because that the upper reference tilt is bounded by 4.5 km ARL height. In all WSR-88D VCPs, the bottom of the 2nd tilt is at $\sim 1^\circ$. The 4.5 km ARL height intersects this elevation angle at ~ 160 km of range (Fig. 4). Therefore VDZ parameter can only be used for ranges shorter than 160 km for reflectivity QC in the first tilt. For higher tilts, the maximum range for a valid VDZ parameter is even shorter. This constraint limits the usefulness of the vertical reflectivity consistency check. But the constraint is necessary for preventing the QC procedure to remove shallow stratiform precipitation echoes at the long ranges. Additional information such as satellite observations can be used to remove clutter in these regions.

The procedures described in sections 2.2.1 to 2.2.4 are repeated for all the tilts except for the highest one (see section 2.2.5) in a volume scan. The process starts from the lowest tilt and progresses upward. Since reflectivities on an upper tilt can be used for QC of reflectivities on lower tilts, any errors in the echo identification on the upper tilt could impact qualities of the reflectivity QC on lower tilts. The bottom to top

approach can avoid this potential downward propagation of erroneous echo identifications.

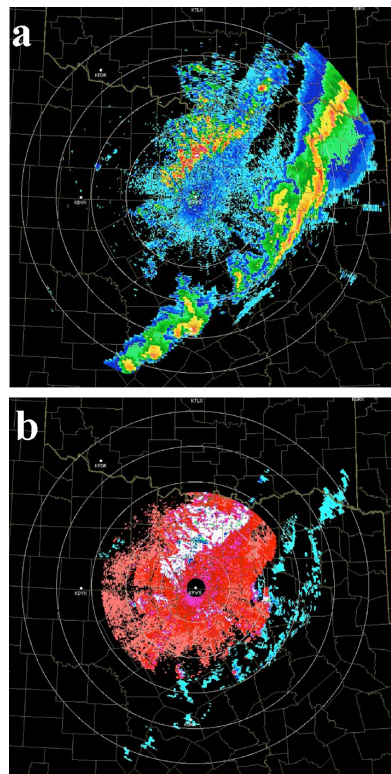


Fig. 5 An example VDZ field (b) and the associated base reflectivity field (a) on 0.5° tilt.

2.2.5 Quality control of the top tilt

Since the calculation of VDZ parameter at a given tilt requires information from upper tilts, it cannot be used for reflectivity quality controls in the highest tilt of a volume scan. In this case, only reflectivity texture field is used in the QC procedure. If the texture value at any given gate is greater than the threshold (a default value of 35 dBZ^2), then the reflectivity observation at the gate is considered a non-precipitation echo and is removed.

3. CASE STUDY

The current reflectivity quality control algorithm has been extensively tested using about 200 volume scans of base data from different radar sites and from different times (seasonal and diurnal). The algorithm performs very well in majority of cases ($> 90\%$). Below are examples of reflectivity fields before and after the QC for various cases.

3.1 Stratiform Rain With Birds Echoes

Radar: KTLX (Twin Lakes, OK)

Date: 05/04/99
Time: 0704 UTC

Stratiform precipitation is seen to the East of the radar (Fig.7). Birds' echoes surround the radar behind the precipitation region. The precipitation echoes are relatively deep (echo top > 5 km). The QC algorithm is very successful in removing the birds' echoes in this case and the *VDZ* field played a critical role.

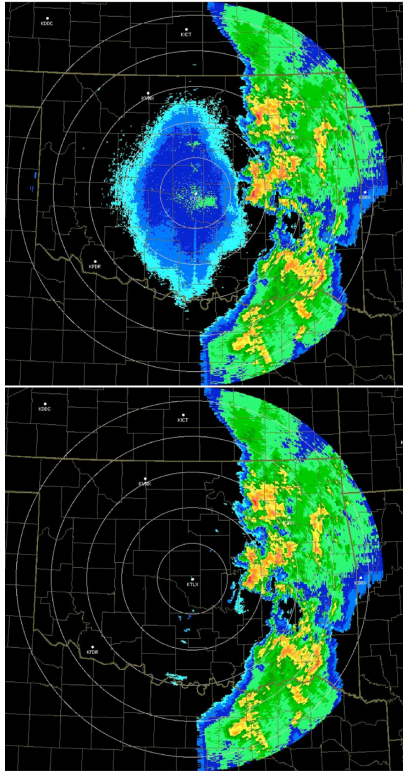


Fig. 6 The first tilt reflectivity before (upper panel) and after (lower panel) the QC.

3.2 Mixed Convective And Stratiform Rain And Clear Air/Biological Echoes

Radar: KTLX (Twin Lakes, OK)
Date: 05/13/04
Time: 1439 UTC

The challenge for the QC of this case is to remove the clear/biological echoes (noisy, light blue reflectivities) around the radar while retaining a small cluster of convective echoes to the southwest of the radar (Fig. 7). The result showed that the QC algorithm performed well in this regard.

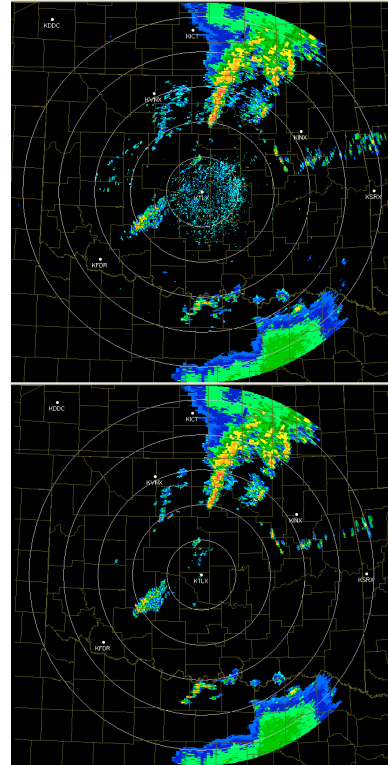


Fig. 7 The first tilt reflectivity before (upper panel) and after (lower panel) the QC.

3.3 AP

Radar: KFWS (Fort Worth, TX)
Date: 04/20/95
Time: 0453 UTC

Extensive AP echo surrounds the radar and is also seen to the North of the radar (Fig. 8). Nearest to the radar, significant echo is still present in the second tilt and some of the AP at further range is associated with significant velocity. Therefore, distinguishing AP from the precipitation to the east is a challenge. In addition, it is essential to retain the complete structure of high reflectivity cells embedded in the squall line. The *VDZ* provided some useful information regarding the nature of the echo and majority of the AP echoes near the radar are successfully removed. However, the *VDZ* parameter is not useful for the longer ranges. A significant amount of AP echoes is left after the QC (the echoes to the North-Northeast of the radar and to the west of the northern end of the squall line, Fig.10). A few scattered high reflectivity clutter near the radar were left because they have vertical continuity up to 3 km ARL height and higher. Additional information, such as that from satellite imagery data, will be used to remove these residual AP clutter.

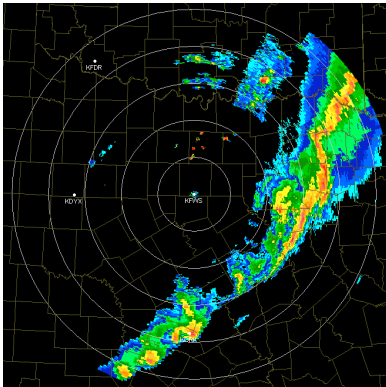
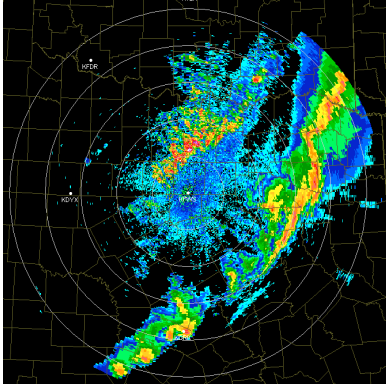


Fig. 8 The first tilt reflectivity before (upper panel) and after (lower panel) the QC.

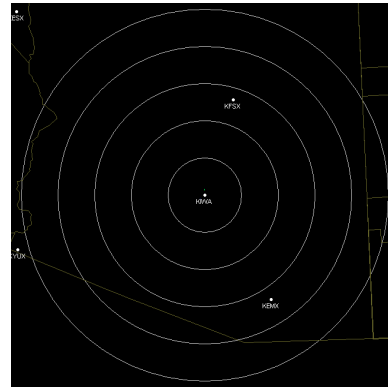
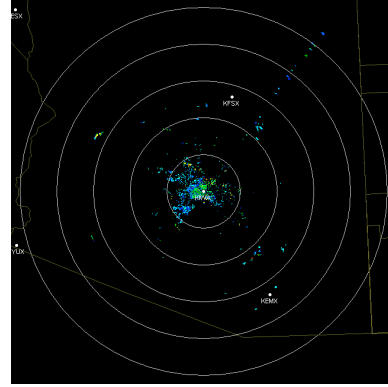


Fig. 9 The first tilt reflectivity before (left panel) and after (right panel) the QC.

3.4 Clear Air Return

Radar: KIWA (Phoenix, AZ)
Date: 02/06/04
Time: 1506 UTC

In clear air, a speckled reflectivity field is observed around the radar, with values ranging from ~10 – 35 dBZ (Fig. 9). The echo appears in early to late morning and is likely results from refractive index gradients in the presence of a shallow nocturnal inversion. Turbulence within the boundary layer creates fluctuations in temperature and humidity leading to changes in the refractive index. This may cause the radar beam to intercept trees, building or even the ground. The noise filter and the *TDBZ* parameter played important roles in removing these non-precipitation echoes.

3.5 Outflow Boundary

Radar: KTLX (Twin Lakes, OK)
Date: 05/08/03
Time: 2201 UTC

In this case an outflow boundary results in a line of echo to the west-southwest of the radar (Fig.10). Insect and/or particulates are concentrated by the outflow and return power to the radar. Due to the shallowness of the echoes, they were identified as non-precipitation echo based on the *VDZ* criteria and were removed from the reflectivity field after QC (Fig.10). For precipitation estimation algorithm this is a desired feature of QC algorithms. But it is noteworthy that new storms are often triggered along these outflow boundaries. Therefore removing these echoes may not be a desired feature for convective initiation applications.

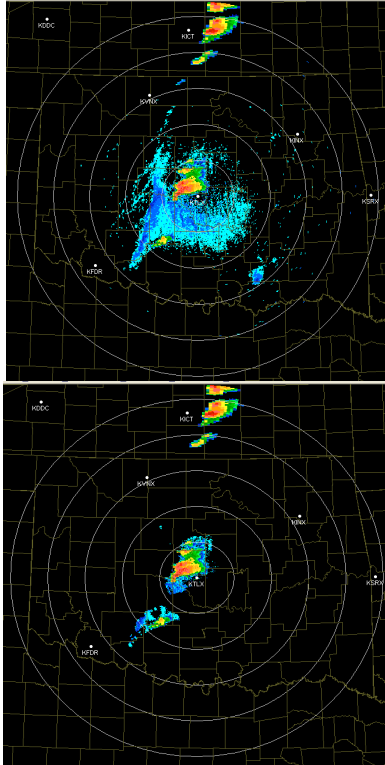


Fig. 10 The first tilt reflectivity before (left panel) and after (right panel) the QC.

3.6 Precipitation At Long Range

Radar: KFSX (Flagstaff, AZ)

Date: 09/24/03

Time: 1654 UTC

In this case, stratiform precipitation is seen at long range (Fig.11). Very little reflectivity is seen in the second tilt and it is not in the same locale as the echo in the first tilt. This is a challenge for QC, as vertical reflectivity checks could lead to the removal of precipitating echo. The QC algorithm successfully retained the precipitation echoes indicating that *TDBZ* and *VDZ* identified areas of precipitation well. The 4.5 km ARL height constraint helped save the echoes at very far ranges.

This case also shows an example of the radar beam ducting and intercepting mountains (The White Mountains) to the southeast of the radar. This cluster of reflectivity slightly higher than other observed echo is AP and ideally should be removed by QC. However, since the region is beyond the range constraint for the *VDZ* parameter, the AP echoes are not removed. This is a very challenging situation and satellite data cannot help due to the fact that there are clouds and precipitation in the same region. Terrain data combined

with time series of reflectivity may help identify these types of AP echoes correctly.

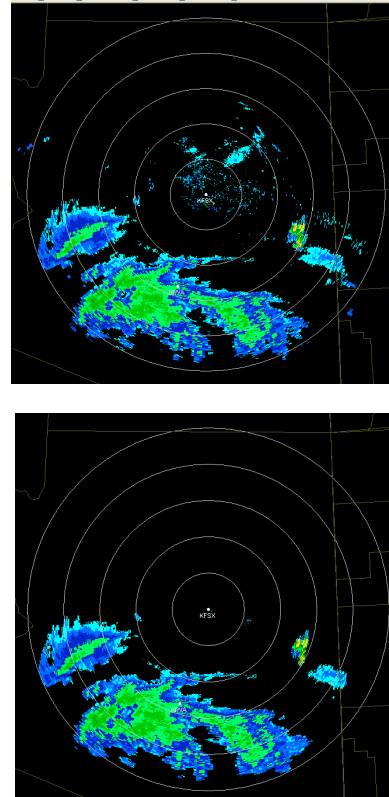


Fig. 11 The first tilt reflectivity before (left panel) and after (right panel) the QC.

4. SUMMARY

A reflectivity quality control algorithm has been developed for identifying and removing non-precipitation echoes from the WSR-88D base reflectivity fields. The algorithm assumes that precipitation and non-precipitation echoes have different horizontal and vertical reflectivity structures. Two main parameters, vertical difference of reflectivity (*VDZ*) and horizontal texture of reflectivity (*TDBZ*), and a set of physically based rules and criteria are developed for the QC algorithm.

The reflectivity QC algorithm has been extensively tested using about 200 volume scans of base level data from different radar sites and from different seasonal and diurnal times. Results have shown that the reflectivity QC algorithm is very successful in identifying non-precipitation echoes such as ground clutter (under both normal and anomalous propagation conditions), clear air and insect echoes, and birds' echoes. These non-precipitation echoes consists more than 90% of the non-precipitation echoes in the WSR-88D reflectivity data. These echoes, if not removed, will contaminate

meteorological products derived from the radar data. By applying the QC algorithm, these noises are largely removed and the resultant reflectivity data can provide “cleaner” and more accurate weather products.

The current reflectivity QC algorithm uses only three-dimensional reflectivity data. The advantage is that the algorithm is relatively simple and highly efficient. Thus it is very suited for operational applications. There are a couple of issues remain to be addressed. One of the issues is that AP clutter at long ranges is sometimes hard to be separated from the shallow stratiform precipitation echoes, especially when the AP clutter shows smooth texture in reflectivity field. A study is currently undergoing in which satellite imagery data, terrain information, and time series of reflectivity are used to further distinguish non-meteorological echoes from meteorological echoes on the bases of the current QC algorithm. Polarimetric radar research has shown promising results on echo classifications, and future efforts will include the integration of polarimetric radar data in the reflectivity QC process.

Acknowledgements

Major funding for this research was provided under the Aviation Weather Research Program NAPDT (NEXRAD Algorithms Product Development Team)

MOU and partial funding was provided under NOAA-OU Cooperative Agreement #NA17RJ1227 and through the collaboration with the Central Weather Bureau of Taiwan, Republic of China.

This research is in response to requirements and funding by the Federal Aviation Administration (FAA). The views expressed are those of the authors and do not necessarily represent the official policy or position of the FAA.

References

- Kessinger et. al., 2003: The radar echo classifier: a fuzzy logic algorithm for WSR-88D, 3rd Conference on Artificial Intelligence Applications to the Environmental Science, AMS, 9-13 February 2003, Long Beach, CA.
- Lakshmanan, V., 2003: Quality control of WSR-88D data. *Preprints for 31st Radar Conference*. Amer. Meteor. Soc., Seattle, WA. 522-525.
- Steiner, M. and J. Smith, 2003: Use of three-dimensional reflectivity structure for automated detection and removal of non-precipitation echoes in radar data. *J. Atmos. Ocea. Tech.*, **19**, 673-686.